The 40 cm remote-controlled telescope Meade LX200ACF of the Shumen Astronomical Observatory

D. Kjurkchieva[1], D. Marchev[1], B. Borisov[1], S. Ibryamov[1], D. Dimitrov[2,1], V. Popov[1], Al. Milev[3], N. Petrov[2]

[1] Department of Physics and Astronomy, Shumen University, 115 Universitetska, 9700 Shumen, Bulgaria

[2] Institute of Astronomy and NAO, Bulgarian Academy of Sciences, Tsarigradsko shossee 72, 1784 Sofia, Bulgaria

[3] Department of Computer systems and Technologies, Shumen University, 115 Universitetska, 9700 Shumen, Bulgaria

d.kyurkchieva@shu.bg

(Submitted on 17.09.2019; Accepted on 9.10.2019)

Abstract. We present the 40 cm telescope of the Shumen Astronomical Observatory and its equipment allowing remote-controlled observations. We found that the unit is appropriate for observations of different types of stars up to 15 mag with precision better than 0.02 mag for short exposures. The fainter stars would require exposures of order of several minutes. The additional autoguiding system of the 40 cm telescope allows prolonged patrols of variable stars as well as long exposures. We determine the transformation equations for transfer to standard Sloan g', r', i' photometric system. Finally, the paper presents the first multicolor light curve obtained by the fully remote-controlled 40 cm telescope during one night. The observed target was the W UMa star GSC 04263-00881 with a period of around 6 hrs.

Key words: instrumentation – telescopes; detectors; site testing; techniques – photometric (transformation coefficients)

Introduction

The Astronomical Observatory of Shumen University (AOShU) is the newest one in Bulgaria (Kjurkchieva 2017). There are two telescopes for professional astronomical observations whose first light was at the end of 2017 (Kjurkchieva 2019).

This paper presents information about the equipment of the 40 cm telescope, the realization of remote control and the first results based on observations by this unit.

1. The 40 cm telescope and its equipment

The 40 cm reflector Meade LX200ACF (Fig. 1) is located in a 5.5 m Scope-Dome. The fork type mount is fixed on a custom build pier especially designed for the observatory latitude. Additional mechanical device provides the fine adjustment of the telescope pier (Fig. 2).

The diameter of the main mirror of the telescope is 40 cm. Its focal length is 4064 mm with a relative aperture f/10. The main detector is a CCD camera FLI PL09000 (3056 × 3056 pixels, 12 × 12 μm/pixel). The field of view is 30 × 30 arcmin and the corresponding resolution is 0.61 arcsec/pixel.

The telescope is equipped with a CFW4-5 filter wheel with squared 50-mm Sloan filters g', r', i', as well as narrow-band filters $H\alpha$ and red continuum ($RedCont$). The narrow-band Sloan filters will be used for searching for emission objects (Dimitrov & Kjurkchieva 2012).

The own focuser of the 40 cm telescope Meade LX200ACF was not enough powerful to support the heavy combination of the CCD camera FLI PL09000 and filter wheel CFW4-5. That is why a new focuser FLI PDF was connected to the telescope by special ring-adapters. It provides computerized focusing of the telescope.

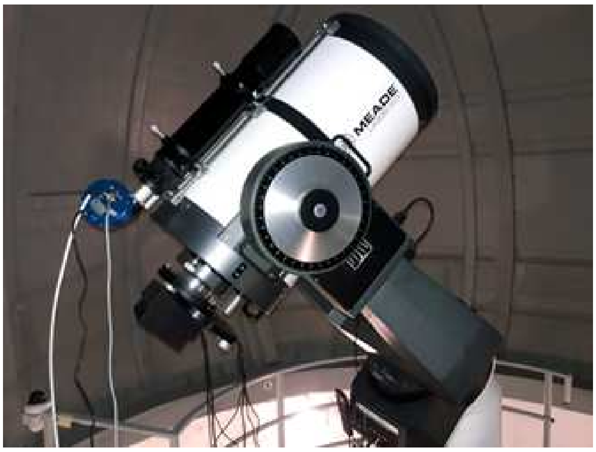

Fig. 1. The 40 cm telescope Meade LX200ACF.

We realized the autoguiding of the telescope by an additional small telescope TS-Optics Guiding Scope 80/600 mm (Fig. 1) with adjustable tube rings and ATIK Titan CCD camera (659 × 494 pixels, 7.4 × 7.4 μm/pixel, minimum exposure length 1/1000 s, Cooling: Termoelectric set point with max ΔT = -20°). The field of view is 28 × 21 arcmin and the corresponding resolution is 2.54 arcsec/pixel.

2. Remote control

The remote control of the telescopes gives a possibility for more effective usage of the observational time and saving of human time, efforts and financial resources (Iliev 2014).

Remote-controlled small telescopes have provided the huge ground-based wide-field surveys: ASAS (Pojmanski 1997), ROTSE (Akerlof 2005), SuperWASP (Pollacco et al. 2006), CRTS (Drake et al. 2014), etc. They are able to discover variable stars, exoplanets, transient and other interesting celestial objects, as well as to carry out follow-up observations of most of them.

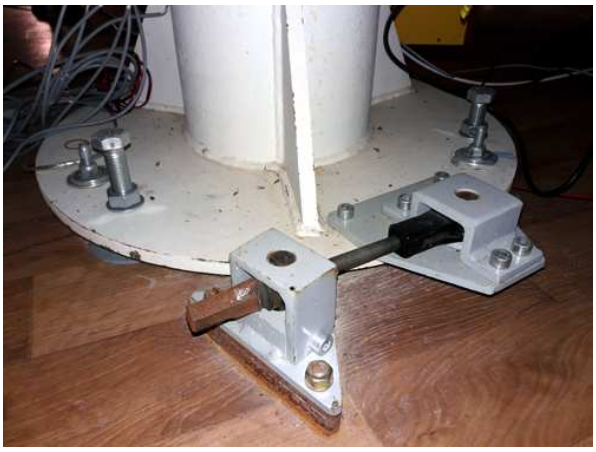

Fig. 2. The mechanical device for fine adjustment of the telescope column.

The realization of the remote control of our 40 cm telescope was the main goal of our work after the first test of the equipment. It included several steps.

We installed the software *TheSky10Pro* and *FocusMax* for connecting, controlling and operating the optical system and the dome.

The telescope-to-dome connection was performed and tested by the standard *ScopeDome* software.

Initially we carried out testing of the remote control of the telescope, dome, CCD camera, filter wheel, focuser and autoguiding separately. Finally, the remote control of the whole equipment was tested.

Due to bad connection between the driving computer and CCD camera by using 25-m USB cable we put the computer into small box with heating system inside the 5.5 m dome.

The power supplies of the equipment components are connected to a computer controlled power switch *Expert Power Control 8210*. A remote-controlled security video camera allows instant inside dome video control. Moreover, outside generator P12000 400V 50HZ (THE SILENT POWER) with AVR equipment provides electricity in case of accidental events (Kjurkchieva et al. 2019).

An automatic weather station *Bresser 7002600* and a Cloud detector *AAG CloudWatcher* and *Starlight Xpress Camera All-Sky Oculus 180 Mono* outside the dome give information about the atmospheric conditions: sky glow and existence of clouds and rain.

Nowadays, *TeamViewer* is used for remote connection with the observatory and telescope.

3. Test observations

Figure 3 illustrates test observations with our 40 cm telescope.

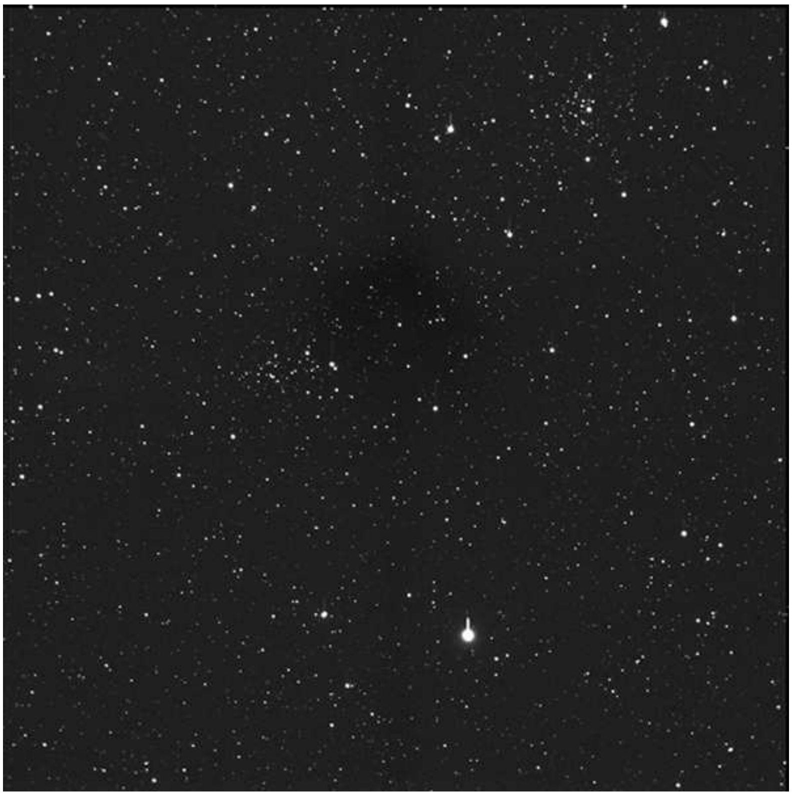

Fig. 3. The open cluster NGC 7790; Date 18.02.2019; Exp. 60 s; Filter: r'

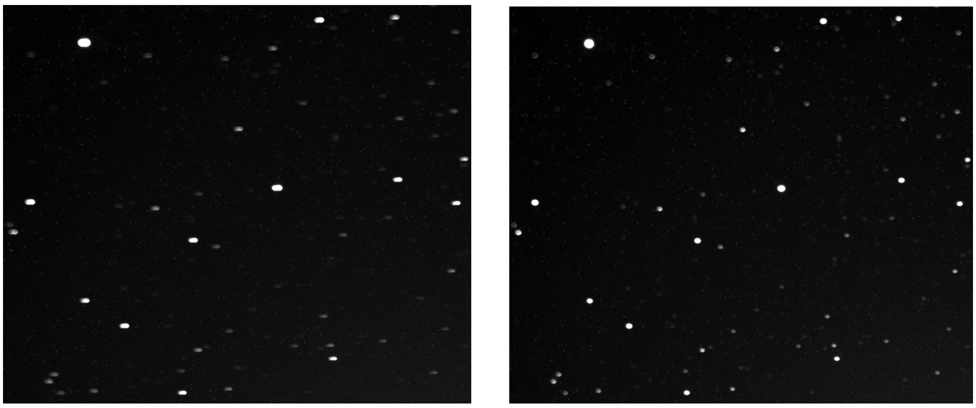

Fig. 4. The same field observed with exposure 60 s both without and by autoguiding.

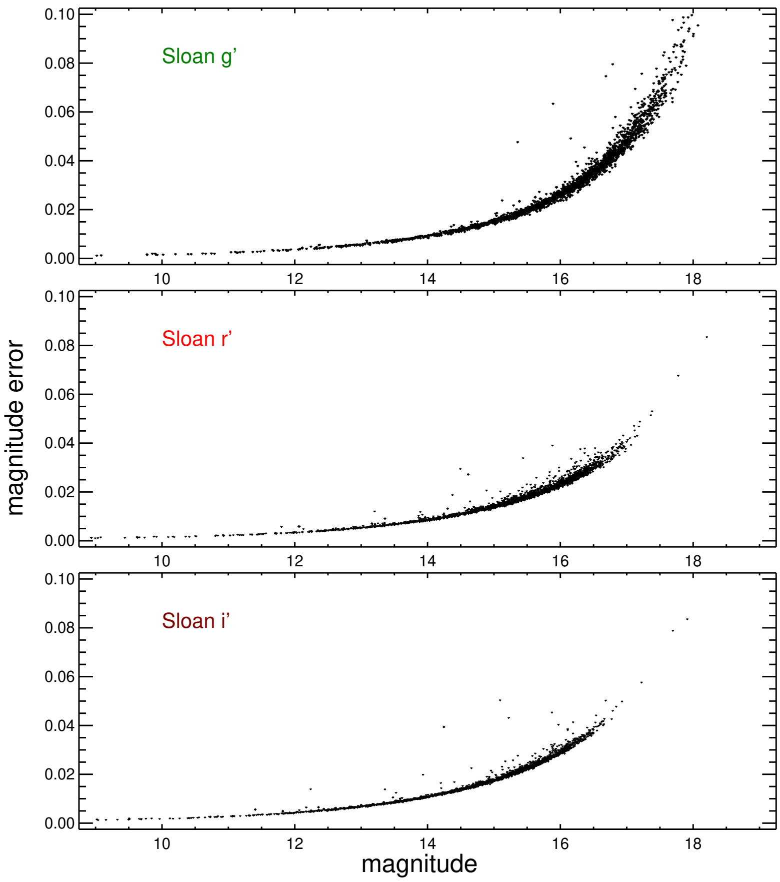

Fig. 5. Dependence of the magnitude precision on the magnitude in different filters

The typical seing (during photometric night but not ideal atmospheric conditions) is around 2 arcsec. Hence, our equipment is appropriate for different tasks requiring star observations. The images of extended objects could be used for student education or popularization goals.

Figure 4 demonstrates the effect of the autoguiding for observations of faint objects requiring long exposures. It is visible that even exposures of 60 s without autoguiding lead to elongated star images.

Figure 5 reveals dependence of the magnitude precision on the magnitude in different filters. It indicates that our equipment is appropriate for observations of stars up to 15 mag with satisfactory precision (0.015 mag).

Figure 6 illustrates the change of image quality from the center to the edges of the field due to the distortions of the optical system.

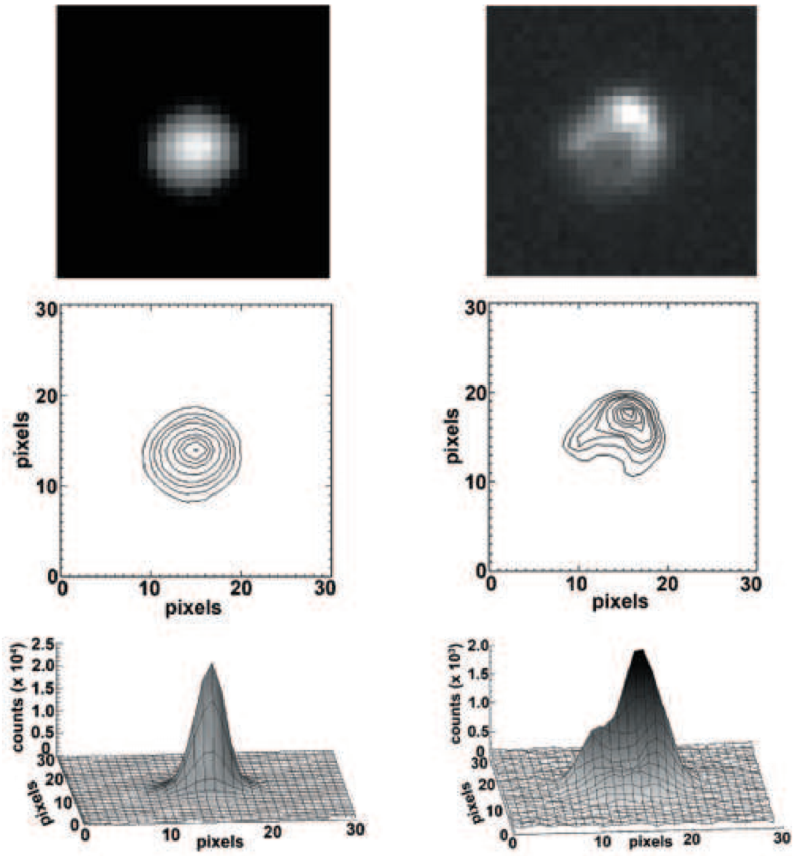

Fig. 6. Stellar images around the center (left) and edge of the frame (right).

4. Transformation coefficients

Each telescope, filter and CCD combination has its own unique characteristics, which, depending on the color of the star being measured and the filters used, can result in magnitude differences of anywhere from several hundredths of a magnitude to several tenths of a magnitude from one observatory to another. By transforming the data to a standardized system, these differences can be greatly reduced if not eliminated.

In order to obtain the transformation equations of our equipment we carried out observations of the field shown in Fig. 3 on Feb 18 2019 with exposures of 20 s. The final images were obtained by stacking of individual images. The measurement of the instrumental magnitudes g_i', r_i', i_i' of 36 stars in the field whose standardized Sloan magnitudes g', r', i' were taken from APASS DR9 (Henden et al. 2016) led to the following transformation equations (Fig. 7):

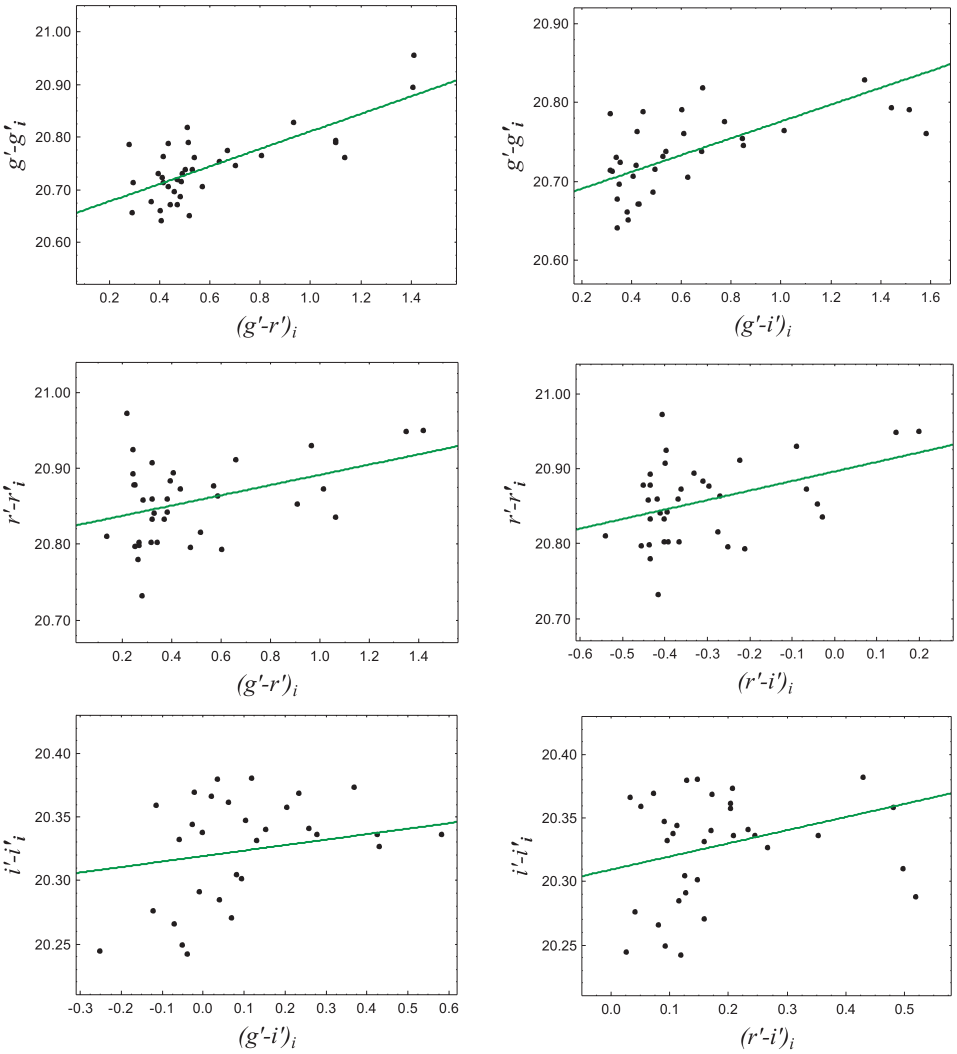

Fig. 7. Diagrams for determination of the transformation equations

$$g' = g'_i + 20.644 + 0.167 * (g' - r')_i \tag{1}$$

$$g' = g'_i + 20.669 + 0.107 * (g' - i')_i \tag{2}$$

$$r' = r'_i + 20.824 + 0.067 * (g' - r')_i \tag{3}$$

$$r' = r'_i + 20.897 + 0.127 * (r' - i') \quad (4)$$

$$i' = i'_i + 20.319 + 0.043 * (g' - i')_i \quad (5)$$

$$i' = i'_i + 20.309 + 0.103 * (r' - i')_i. \quad (6)$$

The errors of the calculated transformation coefficients are of the order of 0.001.

We plan to derive the transformation equations at least once a year or after change of anything in the optical system.

Table 1. Coordinates and magnitudes of the target and standard stars

label	2MASS ID	RA2000	DEC2000	i' [mag]	g' [mag]
Var	J22084858+6057034	22 08 48.6	+60 57 03.4	12.577	14.087
St1	J22080861+6057359	22 08 08.6	+60 57 35.9	12.746	14.625
St2	J22083527+6055380	22 08 35.3	+60 55 38.1	12.173	14.156
St3	J22081815+6059255	22 08 18.2	+60 59 25.6	12.534	13.358
St4	J22090430+6055452	22 09 04.3	+60 55 45.3	13.078	13.417
St5	J22091254+6103595	22 09 12.6	+61 03 59.5	12.436	13.226
St6	J22091830+6048592	22 09 18.3	+60 48 59.3	11.815	13.697
St7	J22093337+6047009	22 09 33.4	+60 47 01.0	12.131	14.281

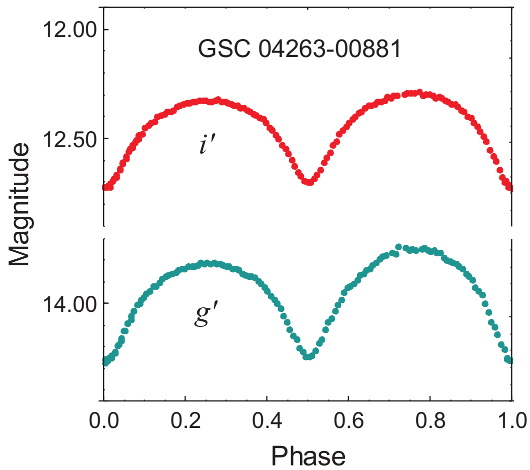

Fig. 8. The folded light curves of GSC 04263-00881 in g' and i' filters from Aug 28 2019

5. First results

The W UMa star GSC 04263-00881 was the first object of scientific observations with the 40 cm telescope and its equipment. Its short-period of around 6 hrs ($P = 0.2615125$ d, Lapukhin et al. 2018) allowed covering the whole orbital cycle during one night.

GSC 04263-00881 was observed on 28 Aug 2019. The atmospheric conditions were good: clear sky, temperature 25 C, humidity 50 %. The CCD was cooled to -20 C. There was no wind and Moon. The exposures in g' and i' filter were respectively 90 s and 60 s. The FWHM of the target images were around 3 pix in g' and 4 pix in i'.

The standard procedure was used for the reduction of the photometric data (de-biasing, dark frame subtraction and flat-fielding) using the software MaxImDL 6.

We performed differential photometry using 7 standard stars. Their magnitudes (Table 2) were taken from the catalogue APASS DR9 (Henden et al. 2016). We transformed the data using equations 2 and 5 and obtained the first precise multicolor light curve of GSC 04263-00881.

In order to obtain the initial epoch of the target we made time-series analysis of our photometric data using Period04 (Lenz & Breger 2005).

The phased data by the obtained ephemeride

$$JD = 2458724.301 + 0.2615125 * E \quad (7)$$

are shown in Fig. 8.

6. Conclusion

The main results from our testing and first star observations with the 40 cm telescope of the Shumen Astronomical Observatory are as follows.

(i) We found that the unit is appropriate for observations of different types of stars up to 15 mag with precision better than 0.02 mag for short exposures (up to a minute). The fainter stars would require prolonged exposures (of order of several minutes).

(ii) The equipment gives a possibility for prolonged patrols of variable stars as well as long exposures due to the autoguiding system.

(iii) We determined transformation equations allowing transfer to standard Sloan g', r', i' photometric system.

(iv) The paper presents the first multicolor light curve obtained by the fully remote-controlled 40 cm telescope during one night. It belongs to the W UMa star GSC 04263-00881 with a period of around 6 hrs.

Acknowledgements. The research was supported partly by projects DN 08-20/2016 and DN 08-01/2016 of Scientific Foundation of the Bulgarian Ministry of Education and Science, project D01-157/28.08.2018 of the Bulgarian Ministry of Education and science, as well as by projects RD-08-92/2019 and RD-08-37/2019 of Shumen University. The authors are grateful to the anonymous referee for the valuable recommendations.

References

Akerlof, C., 2005, MPC, 54971, 10
Dimitrov, D., Kyurkchieva, D., 2012, BlgAJ, 18, 63
Drake, A.J., Djorgovski, S.G., Garcia-Álvarez, D., Graham, M.J., Catelan, M. et al., 2014, ApJ, 790, 157
Henden, A.A. Templeton, M., Terrell, D.; Smith, T. C.; Levine, S., Welch, D.,2016, yCat 2336
Iliev, I., 2014, CoSka, 43, 169
Kjurkchieva, D., 2017, Astronomical Calendare 2018, ISSN 0861-1270, p. 87
Kjurkchieva, D., Ibryamov, S., Borisov, B., Marchev, D., Popov, V., Dimitrov, D., 2019, BAJ, 31, 30
Lapukhin, E. G.; Veselkov, S. A.; Zubareva, A. M. , 2018, PZP, 18, 2
Lenz, P., Breger, M., 2005, CoAst, 146, 53
Pojmanski, G., 1997, AcA, 47, 467
Pollacco, D. L.; Skillen, I.; Collier Cameron, A.; Christian, D. J.; Hellier, C. et al., 2006, PASP, 118, 1407